Open access • Journal Article • DOI:10.1039/C7CP07843A

A combined theoretical and experimental investigation of the kinetics and dynamics of the O(1D) + D2 reaction at low temperature. — Source link

Dianailys Nuñez-Reyes, Kevin M. Hickson, Kevin M. Hickson, Pascal Larrégaray ...+6 more authors

Institutions: University of Bordeaux, Centre national de la recherche scientifique, Spanish National Research Council, The Cyprus Institute ...+1 more institutions

Published on: 07 Feb 2018 - Physical Chemistry Chemical Physics (The Royal Society of Chemistry)

Topics: Reaction dynamics, Molecular dynamics, Quantum state and Reaction rate constant

Physical Chemistry Chemical Physics c7cp07843a

We have presented the Graphical Abstract text and image for your article below. This brief summary of your work will appear in the contents pages of the issue in which your article appears.

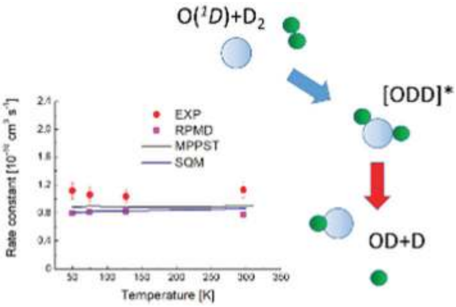

A combined theoretical and experimental investigation of the kinetics and dynamics of the $O(^1D)$ + D_2 reaction at low temperature Q2

Dianailys Nuñez-Reyes, Kevin M. Hickson,
Pascal Larrégaray, Laurent Bonnet,
Tomás González-Lezana and Yury V. Suleimanov Q3

Rate constant calculations by the MPPST, SQM and RPMD methods accurately reproduce the measured values down to low temperature.

Please check this proof carefully. **Our staff will not read it in detail after you have returned it.**

Proof corrections must be returned as a single set of corrections, approved by all co-authors. No further corrections can be made after you have submitted your proof corrections as we will publish your article online as soon as possible after they are received.

Please ensure that:

- The spelling and format of all author names and affiliations are checked carefully. Names will be indexed and cited as shown on the proof, so these must be correct.
- Any funding bodies have been acknowledged appropriately.
- All of the editor's queries are answered.
- Any necessary attachments, such as updated images or ESI files, are provided.

Translation errors between word-processor files and typesetting systems can occur so the whole proof needs to be read. Please pay particular attention to: tables; equations; numerical data; figures and graphics; and references.

Please send your corrections preferably as a copy of the proof PDF with electronic notes attached or alternatively as a list of corrections – do not change the text within the PDF file or send a revised manuscript. Corrections at this stage should be minor and not involve extensive changes.

Please return your **final** corrections, where possible within **48 hours** of receipt, by e-mail to: pccp@rsc.org. If you require more time, please notify us by email.

Funder information

Providing accurate funding information will enable us to help you comply with your funders' reporting mandates. Clear acknowledgement of funder support is an important consideration in funding evaluation and can increase your chances of securing funding in the future. We work closely with Crossref to make your research discoverable through the Funding Data search tool (http://search.crossref.org/funding).

Further information on how to acknowledge your funders can be found on our webpage (http://rsc.li/funding-info).

What is Funding Data?

Funding Data (http://www.crossref.org/fundingdata/) provides a reliable way to track the impact of the work that funders support. We collect funding information from our authors and match this information to funders listed in the Crossref Funder Registry. Once an article has been matched to its funders, it is discoverable through Crossref's search interface.

PubMed Central

Accurate funder information will also help us identify articles that are mandated to be deposited in PubMed Central (PMC) and deposit these on your behalf.

Providing funder information

We have combined the information you gave us on submission with the information in your acknowledgements. This will help ensure funding information is as complete as possible and matches funders listed in the Crossref Funder Registry. **Please check that the funder names and grant numbers in the table are correct.** This table will not be included in your final PDF but we will share the data with Crossref so that your article can be found *via* the Funding Data search tool.

Funder name	**Funder ID (for RSC use only)**	**Award/grant/contract number**
Centre National pour la Recherche Scientifique et Technique	501100006319	Unassigned
Centre National d'Etudes Spatiales	501100002830	Unassigned
Ministerio de Ciencia e Innovación	501100004837	FIS2014-51993-P, FIS2017-83157-P
Research Promotion Foundation	501100001810	Cy-Tera ΝΕΑ ΥΠΟΔΟΜΗ/ΣΤΡΑΤΗ/0308/31
European Cooperation in Science and Technology	501100000921	CM1401

Q1

If a funding organisation you included in your acknowledgements or on submission of your article is not currently listed in the registry it will not appear in the table above. We can only deposit data if funders are already listed in the Crossref Funder Registry, but we will pass all funding information on to Crossref so that additional funders can be included in future.

Researcher information

If any authors have ORCID or ResearcherID details that are not listed below, please provide these with your proof corrections. Please check that the ORCID and ResearcherID details listed below have been assigned to the correct author. Authors should have their own unique ORCID iD and should not use another researcher's, as errors will delay publication.

Please also update your account on our online manuscript submission system to add your ORCID details, which will then be automatically included in all future submissions. See here for step-by-step instructions and more information on author identifiers.

First (given) name(s)	**Last (family) name(s)**	**ResearcherID**	**ORCID**
Dianailys	Nuñez-Reyes		

Kevin M.	Hickson		0000-0001-8317-2606
Pascal	Larrégaray		
Laurent	Bonnet		0000-0002-4022-2826
Tomás	González-Lezana		0000-0003-0010-5219
Yury V.	Suleimanov		

Queries for the attention of the authors

Journal: **PCCP**

Paper: **c7cp07843a**

Title: **A combined theoretical and experimental investigation of the kinetics and dynamics of the $O(^1D) + D_2$ reaction at low temperature**

For your information: You can cite this article before you receive notification of the page numbers by using the following format: (authors), Phys. Chem. Chem. Phys., (year), DOI: 10.1039/c7cp07843a.

Editor's queries are marked on your proof like this Q1, Q2, etc. and for your convenience line numbers are indicated like this 5, 10, 15, ...

Please ensure that all queries are answered when returning your proof corrections so that publication of your article is not delayed.

Query reference	Query	Remarks
Q1	Funder details have been incorporated in the funder table using information provided in the article text. Please check that the funder information in the table is correct.	
Q2	Please confirm that the spelling and format of all author names is correct. Names will be indexed and cited as shown on the proof, so these must be correct. No late corrections can be made.	
Q3	Do you wish to indicate the corresponding author(s)? If so, please specify the corresponding author(s).	
Q4	Do you wish to add an e-mail address for the corresponding author? If so, please provide the relevant information.	
Q5	Please note that a conflict of interest statement is required for all manuscripts. Please read our policy on Conflicts of interest (http://rsc.li/conflicts) and provide a statement with your proof corrections. If no conflicts exist, please state that "There are no conflicts to declare".	

PCCP

PAPER

Cite this: DOI: 10.1039/c7cp07843a

A combined theoretical and experimental investigation of the kinetics and dynamics of the $O(^1D) + D_2$ reaction at low temperature†

Dianailys Nuñez-Reyes,[ab] Kevin M. Hickson,[ab] Pascal Larrégaray,[ab] Laurent Bonnet,[ab] Tomás González-Lezana[c] and Yury V. Suleimanov[de]

Received 21st November 2017, Accepted 17th January 2018

DOI: 10.1039/c7cp07843a

rsc.li/pccp

The $O(^1D) + H_2$ reaction is a prototype for simple atom–diatom insertion type mechanisms considered to involve deep potential wells. While exact quantum mechanical methods can be applied to describe the dynamics, such calculations are challenging given the numerous bound quantum states involved. Consequently, efforts have been made to develop alternative theoretical strategies to portray accurately the reactive process. Here we report an experimental and theoretical investigation of the $O(^1D) + D_2$ reaction over the 50–296 K range. The calculations employ three conceptually different approaches – mean potential phase space theory, the statistical quantum mechanical method and ring polymer molecular dynamics. The calculated rate constants are in excellent agreement over the entire temperature range, exhibiting only weak temperature dependence. The agreement between experiment and theory is also very good, with discrepancies smaller than 26%, thereby validating the hypothesis that long-lived complex formation dominates the reaction dynamics at low temperature.

1 Introduction

Atomic oxygen is an important species in the chemistry of the interstellar medium,[1] in planetary atmospheres[2] and in combustion.[3] Oxygen atoms in their ground triplet state, $O(^3P)$, participate in reactions which contribute to the Ox, NOx, HOx and ClOx budgets of the Earth's atmosphere[4] and radical–radical reactions such as $O(^3P) + OH \rightarrow O_2 + H$ are important for the transformation of atomic to molecular oxygen in interstellar clouds.[5] Although oxygen atoms in their first excited singlet state, $O(^1D)$, are characterized by a long radiative lifetime,[6] it is too short for these atoms to play a meaningful role in the chemistry of the dense interstellar medium. In planetary atmospheres, the photodissociation of oxygen bearing molecules can yield high fractional abundances of $O(^1D)$ atoms. In this respect, excited state atomic oxygen reactions have a clear impact on the overall chemistry. A well-known example is that of the reactions of $O(^1D)$ atoms with H_2O, H_2 and CH_4 reaction above the Earth's tropopause to form hydroxyl radicals that participate in the catalytic destruction of stratospheric ozone. Surprisingly, there are relatively few kinetics measurements of the $O(^1D) + H_2$ reaction and its deuterated counterparts, with most previous experiments having been performed at 300 K.[7–12] Temperature dependent rate constants have been recorded for the $O(^1D) + H_2$ reaction over the combined 50–420 K range,[13–16] but only room temperature values exist for the other isotopologues. In contrast, the dynamical aspects of the $O(^1D) + H_2$ reaction and its deuterated counterparts have been studied experimentally[17–27] and theoretically[18,20–22,28–47] on numerous occasions due to their fundamental importance as examples of atom–diatom insertion reactions involving deep potential wells. As large numbers of bound quantum states are supported in these systems, the application of exact quantum mechanical (QM) methods is computationally expensive, particularly when several potential energy surfaces (PESs) are involved. As a result, considerable effort has been devoted to finding approximate theoretical strategies which might adequately describe the dynamics of these systems.

---

[a] Université de Bordeaux, Institut des Sciences Moléculaires, F-33400 Talence, France

[b] CNRS, Institut des Sciences Moléculaires, F-33400 Talence, France

[c] Instituto de Física Fundamental, CSIC, IFF-CSIC Serrano 123, 28006 Madrid, Spain

[d] Computation-based Science and Technology Research Center, Cyprus Institute, 20 Kavafi Str., Nicosia 2121, Cyprus

[e] Department of Chemical Engineering, Massachusetts Institute of Technology, 77 Massachusetts Ave., Cambridge, Massachusetts 02139, USA

† Electronic supplementary information (ESI) available: Intermediate RPMD data such as the profiles of potential of mean force (Fig. S1) and transmission coefficients (Fig. S2). Experimental second-order plots recorded at 127 K and 75 K (Fig. S3). The input parameters for the RPMD rate calculations for both potential energy surfaces ($^1A'$ and $^1A''$) (Table S1). Final thermal RPMD rate constants and ring polymer recrossing factors plateau values (Table S2). The measured second-order rate constants (Table S3). See DOI: 10.1039/c7cp07843a

One relatively simple approach that could be applied to such systems is Mean Potential Phase Space Theory (MPPST).[48] It relies on the assumption of complex-forming dynamics for the reaction, the states of the intermediate complex being statistically populated. Dynamical observables are then predicted from the calculation of individual capture probabilities from the reactant and product states. In MPPST, the inter-fragment interaction is averaged over the Jacobi angle. It is thus assumed to be isotropic so that capture probabilities can be described by semi-classical two-body capture models,[49] including quantization of reactant/product states and tunneling through centrifugal barriers.[50,51]

The statistical quantum method (SQM),[52] also developed under the assumption of complex-forming dynamics for the reaction, involves the calculation of individual capture probabilities by means of rigorous QM techniques on full *ab initio* PESs. The application of both MPPST and SQM to a large list of atom–diatom reactions[53] have revealed their capabilities to reproduce the main dynamical features observed both in experiments and exact QM studies, thus showing the role played by insertion mechanisms in the overall dynamics of the corresponding reactive processes.

Ring polymer molecular dynamics (RPMD) rate theory is an alternative approach that has been developed[54] and extensively benchmarked[16,55–73] over the past decade. It is based on the classical isomorphism between a quantum system and its n classical copies forming a necklace and coupled to its nearest neighbors *via* harmonic interactions. The real-time classical dynamics of this necklace 'ring polymer' represents an *ad hoc* idea of RPMD[54,55] to calculate approximately real-time correlation functions responsible for describing various dynamical processes, including chemical reactions.[56–58] Extensive studies of elementary gas-phase reactions have shown[56] that such approximations allow QM effects of nuclear motions to be captured precisely, providing reliable and accurate estimates of thermal rate constants for different energy profiles along chemical reaction paths and over a wide range of temperatures.

In this paper, we report a combined experimental and theoretical investigation of the $O(^1D) + D_2$ reaction at low temperature. There has been significant debate regarding the dynamical aspects of the $O(^1D) + H_2$ reaction and isotopic variants[53] where reaction is thought to occur predominantly over the ground state $1^1A'$ PES through the formation of an H_2O intermediate, 703 kJ mol^{-1} below the reagent level. The precise roles played by excited electronic states in different energy regimes are thought to be relevant considerations to distinguish the mechanisms governing the overall reaction dynamics. In a previous study of the $O(^1D) + H_2$ reaction,[16] thermal rate constants derived by the RPMD method over the $1^1A'$ and $1^1A''$ PESs were shown to be in reasonably good agreement with measured values down to 50 K. As the $1^1A''$ surface was shown to contribute negligibly to the overall reactivity below room temperature, these authors hypothesized that the difference between measurements and the RPMD results could be due to coupling between the $1^1A'$ and $2^1A'$ states. Indeed, precise QM wave packet (WP) calculations[44] of the $O(^1D) + H_2$ system have suggested that this nonadiabatic pathway could contribute significantly to the overall reactivity. For the $O(^1D) + D_2$ reaction, an analysis of OD product distributions from H(D)-Rydberg 'tagging' time-of-flight experiments[28] at collision energies within the range 2.0–3.2 kcal mol^{-1} revealed a transition between complex-forming dynamics at lower energy to an abstraction process at higher energy. Similarly, the quasi-classical trajectory (QCT) investigation of Aoiz *et al.*[74] observed an increase in the backward scattering component of the differential cross section (DCS) for increasing collision energies (86.7–138.8 meV); a finding which is indicative of the appearance of an abstraction type mechanism and a larger contribution from the $1^1A''$ PES. In this sense, the experimental results presented here and the comparison with theoretical methods designed to treat complex-forming reactions, constitute a rigorous test of the overall dynamics of the $O(^1D) + D_2$ reaction at low temperature.

On the theoretical side, the MPPST, SQM and RPMD methods were employed to describe the reaction dynamics over the $1^1A'$ PES and to furnish thermal rate constants down to 50 K. RPMD calculations were also performed over the $1^1A''$ PES. In a similar manner to our earlier investigation of the $O(^1D) + H_2$ reaction,[16] these results confirm its negligible contribution to the overall reactivity at room temperature and below. To validate the theoretical approaches, rate constants were measured over the 50–296 K range using a supersonic flow reactor by following the kinetics of $O(^1D)$ loss.[75] Sections 2 and 3 describe respectively the experimental and theoretical methods used in this work. The results are discussed in Section 4 and our conclusions are presented in Section 5.

2 Experimental methods

All measurements were performed using a continuous supersonic flow (Laval nozzle) reactor. The experimental setup has been described in earlier papers,[76,77] while modifications that allowed the kinetics of atom–molecule reactions to be studied are described in more recent work.[16,70,71,75,78–86] In an identical manner to previous investigations of excited state atom reactions,[16,70,71,75,78,81,84–86] only Laval nozzles employing argon were used for these experiments as a result of the fast electronic quenching of $O(^1D)$ atoms by carrier gases such as N_2.[75] These Ar based nozzles allowed uniform supersonic flows to be generated at specified temperatures of 50 K, 75 K and 127 K, with calculated densities in the range $(1.26–2.59) \times 10^{17}$ cm^{-3} and flow velocities between 419 and 505 m s^{-1}. The calculated and measured characteristics of the three nozzles used in this work are given in Table 1 of Grondin *et al.* (2016).[75] In addition to the low temperature experiments, kinetic measurements were also performed at 296 K by removing the Laval nozzle and by reducing the flow velocity, effectively using the apparatus as a slow-flow reactor. Nevertheless, the flow velocity (73 cm s^{-1}) was still high enough to ensure that the gas in the probe region was always replenished between laser shots.

$O(^1D)$ atoms were generated in an identical manner to our other recent studies of $O(^1D)$ reactivity[16,75,85] through the pulsed laser photolysis of ozone (O_3) at 266 nm with an energy of ~23 mJ. $O(^1D)$ atoms were detected through resonant pulsed vacuum ultraviolet laser induced fluorescence (VUV LIF) at 115.215 nm *via* the $O(^1D)$ 3s ^1D–2p ^1D transition. The procedure to generate tunable light at this wavelength by frequency tripling has already been described by Grondin *et al.*[75] Nevertheless, a change in the composition of the rare gas mixture used in the tripling cell (75 Torr of xenon and 155 Torr of argon) was found to yield approximately 30% higher fluorescence signals compared to earlier work using 100 Torr of xenon and 230 Torr of argon. The present VUV LIF collection optics and solar blind photomultiplier tube (PMT) are identical to those used in the recent work of Hickson and Suleimanov.[16]

The output of the PMT was connected to a boxcar integrator for signal processing and acquisition with the acquisition electronics, lasers and oscilloscope being synchronized by a delay generator operating at 10 Hz. Each time point consisted of 30 individual laser shots, with at least 50 time intervals recorded for each $O(^1D)$ decay profile. Time points recorded with the probe laser firing at negative delays with respect to the photolysis laser allowed the pre-photolysis baseline level (consisting mostly of scattered light from the probe laser) to be evaluated.

The gases used in the experiments O_2 (99.999%), Ar (99.999%), D_2 (99.8%) and Xe (99.998%) were not purified prior to use. All flows were controlled by calibrated digital mass flow controllers. To derive rate constants for the $O(^1D) + D_2$ reaction required a precise knowledge of the D_2 concentration in the supersonic flow. This quantity was determined from its flow ratio (F_{D_2}/F_{tot}) multiplied by the calculated total flow density. It was always several orders of magnitude larger than the estimated $O(^1D)$ concentration so that pseudo-first-order conditions could be assumed for all measurements. Due to inefficient gas-phase spin conversion, the D_2 used in the present experiments was characterized by a fixed *ortho*/*para* ratio of 2 : 1 at all temperatures.

3 Theoretical methods

Statistical quantum mechanics

The SQM method has been used before in a series of investigations focused on complex-forming reactions.[52,53,87,88] Assuming that the reaction proceeds *via* the formation of an intermediate species between reagents and products, the state-to-state probability can be approximated using the following expression:[52]

$$\left|S^J_{vj\Omega,v'j'\Omega'}(E)\right|^2 \approx \frac{p^J_{vj\Omega}(E)\cdot p^J_{v'j'\Omega'}(E)}{\sum\limits_{v''j''\Omega''} p^J_{v''j''\Omega''}(E)} \qquad (1)$$

where $vj\Omega$ and $v'j'\Omega'$ refer, respectively, to the initial and final rovibrational state of D_2, indicating the quantum numbers for vibrational, rotational and third component of the angular momentum; the $p^J(E)$ quantities correspond to the probability to form the complex from the initial state at the collision energy E and for the total angular momentum J. The sum in the denominator of eqn (1) runs for all energetically open rovibrational states at the energy E for both reagent and product channels. Using the above expression for the reaction probability, it is then possible to calculate the corresponding integral cross section, $\sigma_{vjv'j'}(E)$ and then the thermal rate constant:

$$k_{vj,v'j'}(T) = \sqrt{\frac{8\beta^3}{\pi\mu}}\int_0^\infty \sigma_{vj,v'j'}(E)\mathrm{e}^{-\beta E}E\mathrm{d}E \qquad (2)$$

where we have defined $\beta = (k_BT)^{-1}$ and the cross section includes the 1/5 factor corresponding to the electronic partition function.

Here, statistical calculations have been performed on the ground $^1A'$ PES of Dobbyn and Knowles[89,90] and the capture probability calculation of eqn (1) has been achieved using the time-independent propagation described in ref. 52 in a region defined between R_c (the distance at which the D_2O complex is supposed to form) and R_{max} (an asymptotic distance) with values 1.9 Å (2.5 Å) and 27.8 Å (36.9 Å), respectively for reagents (products). SQM calculations for both $j = 0$ and $j = 1$ initial rotational states of D_2 have been performed and total cross sections have been calculated considering the usual 2/3 and 1/3 coefficients for the $D_2(j = 0)$ and $D_2(j = 1)$ populations respectively, a ratio which describes reasonably well the actual experimental conditions. The centrifugal sudden approximation[52] provides good enough results in comparison with the coupled-channel version of the SQM approach and it suffices for the presently investigated collision energy range (10^{-5}–0.4 eV).

Mean potential phase space theory

MPPST is based on a semi-classical statistical approach for atom–diatom reaction.[91,92] It uses the same statistical assumptions for the intermediate complex states as the SQM method. However, capture probabilities from the asymptotic semi-classically quantized (v, j, l) states are computed in an approximate manner. For barrierless processes, such as the one studied here, the reactant/product channel anisotropies are expected to be moderate. Consequently, the inter-fragment potential might be assumed to be isotropic: anisotropy is implicitly considered by averaging the *ab initio* PES over the reactant γ Jacobi angle in attractive regions for the $^1A'$ $O(^1D) + D_2$ and OD + D channels.[89,90] Capture probabilities are then computed *via* a two-body capture model[49] accounting for possible tunneling through the radial effective potential through the Wentzel–Kramers–Brillouin (WKB) model[50,51] and used in eqn (1) and (2).[48] A simplified classical mechanical treatment of the orbital angular momentum leads to results in quantitative agreement because of subtle compensation between tunneling and quantum reflection.[51] Besides, as the process is highly exothermic (1.89 eV), the reaction cross-section equals the intermediate complex cross-section so that capture from the reactant is only needed if no information on the dynamical observables of the products is required (as is the case for the rate constant calculations). It should be noted that, because of the isotropic assumption for the inter-fragment potential, the capture cross-section does not depend on the D_2 initial rotational state.

Ring polymer molecular dynamics

In the present study, we used the RPMD rate code developed by one of us (YVS).[93] The RPMD rate computational procedure is well documented in previous studies[57–59] and in a recent review.[56] Briefly, the Bennett–Chandler factorization[94,95] is used to avoid high computational expense of the direct trajectories approach which can be prohibitive at low temperatures and/or high energy barriers. The calculation is split into two steps – the construction of the ring polymer potential of mean force $W(\xi)$ (or free energy) profile along the reaction coordinate ξ defined using the formalism of two dividing surfaces (1)[56,57,59,93] and the ring polymer transmission coefficient κ (or recrossing factor) calculation (2). These steps are usually performed sequentially to detect the maximum value of the free energy during the first step and to initiate the recrossing factor calculations from this point during the second step. This allows recrossings to be minimized (thereby avoiding the issue of converging small values of κ) and the propagation time required to achieve the plateau value of κ to be optimized. For thermally activated energy profiles, the free energy barrier is located near the classical saddle point configuration while for reactions of insertion type it is usually located prior to the complex (deep well) and is due to the entropic factor.[56]

Theoretical RPMD rate constants were obtained using the two lowest PESs $1^1A'$ and $1^1A''$ which possess barrierless and thermally activated energy profiles, respectively. In the present study, we employed the Dobbyn–Knowles surfaces.[89,90] The input parameters are summarized in Table S1 (ESI†) along with the intermediate RPMD results such as the potential of mean force (PMF) (Fig. S1, ESI†) and the transmission coefficient (Fig. S2, ESI†) which are similar to the results previously obtained for the $O(^1D) + H_2$ reaction.[16] PMFs for the $1^1A'$ PES are nearly flat before entering the complex-formation region at long range while for the $1^1A''$ PES they demonstrate free energy barriers due to the thermally activated nature of the title reaction on this excited PES thus explaining why its contribution decreases dramatically with decreasing temperature. Plateau values of the transmission coefficients for the $1^1A''$ PES are achieved much faster (after 0.4 ps, see Fig. S2, ESI†) than for the $1^1A'$ surface for which the transmission coefficients were propagated to longer time (2 ps). This is a characteristic feature of barrierless reactions with a deep well along the reaction path.[56] The final results of the present RPMD calculations are summarized in Table S2 (ESI†).

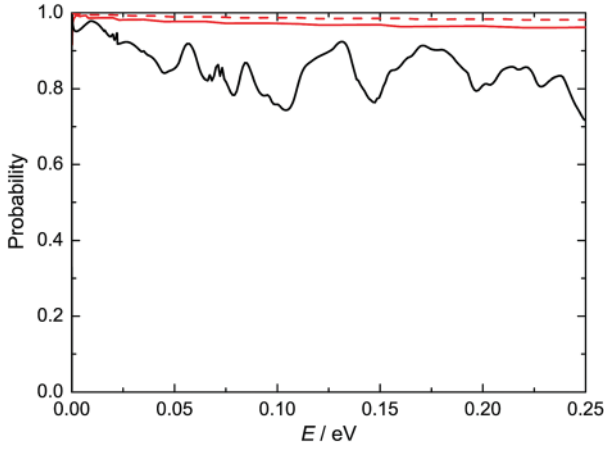

Fig. 1 Total reaction probability for $O(^1D) + D_2$ as a function of the collision energy for zero total angular momentum ($J = 0$) (solid black line) Pradhan *et al.*[96] $O(^1D) + D_2$ ($v = 0$, $j = 0$); (red dashed line) MPPST method, this work; (red solid line) SQM method, this work.

4 Results and discussion

The possible complex-forming character of the $O(^1D) + H_2$ reaction has already been investigated by statistical methods.[45,46,52,53] The calculated rovibrational cross sections and DCSs compared favourably with both exact QM and experimental results at $E_c = 56$ meV, suggesting that the dynamical features observed at this collision energy resulted predominantly from an insertion mechanism. A statistical description of the dynamics below 150 meV was also performed in a previous study of the $O(^1D) + H_2$ reaction, including a comparison of rate constants derived by the SQM and MPPST methods with exact QM and experimental results.[45] An equivalent study can be performed for the $O(^1D) + D_2$ system, comparing statistical predictions with previous work. QM reaction probabilities obtained by Pradhan *et al.*[96] for a zero total angular momentum $J = 0$ using the same $1^1A'$ PES[89,90] are reasonably well described by the MPPST and SQM approaches as can be seen in Fig. 1.

The statistical probabilities of 0.96–0.98 are only slightly above the QM results. In Fig. 2 we present integral cross

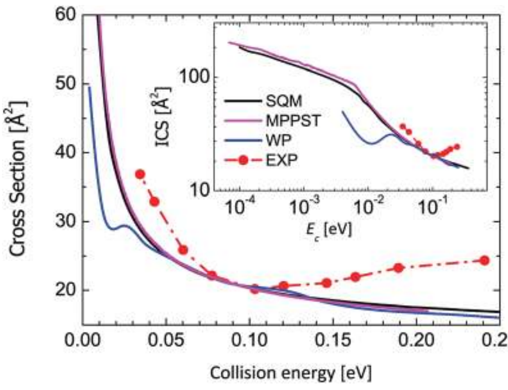

Fig. 2 Integral cross section for the $O(^1D) + D_2$ reaction as a function of the collision energy. (solid black line) SQM method, this work; (solid magenta line) MPPST method, this work; (solid blue line) WP results from Sun *et al.*[101] and experimental cross sections from Hsu *et al.*[23] (red points and dashed line). In the inset the same results on a logarithmic scale down to lower energies.

sections (ICSs) for the title reaction up to ≈0.25 eV collision energy. The WP results by Sun *et al.*[101] and the experimental ICSs reported by Hsu *et al.*[23] are also included for comparison. Whereas both statistical approaches predict cross sections which deviate from the observed behavior exhibited by the measurements of Hsu *et al.*[23] as the energy increases, both SQM and MPPST calculations seem to improve on the apparent deficiencies of the WP values of Sun *et al.*[101] In fact, the extension to low energies (10^{-4} eV) shown in the inset of Fig. 2 reveals that present statistical cross sections display the expected behavior as E_c decreases.

Fig. 3 shows experimental DCSs for the O(^{1}D) + D$_2$ reaction at E_c = 0.104 eV (top panel) and 0.228 eV (bottom panel) taken from Ahmed *et al.*[97] and Alagia *et al.*,[18] respectively.

The corresponding SQM and MPPST angular distributions, also shown, agree well at lower collision energy (see top panel). DCSs calculated with a QCT approach by Rio and Brandao[32] at the same energies (not shown here) were obtained using a different PES[98] and are slightly larger than present statistical distributions. Although measurements were not performed at the forward (90°) and backward (180°) scattering directions, the accord with the theoretical distributions over the rest of the angular range is remarkable. Noticeable deviations are observed however, at higher energy (0.228 eV – bottom panel of Fig. 3). While no definitive statements can be made by comparing the calculated absolute DCSs with a relative angular distribution obtained through a transformation between the laboratory and center of mass reference systems, these differences might be an indication of the onset of an abstraction mechanism as the energy increases that cannot be properly described using the statistical approaches (as seen with the cross sections before). QCT calculations on both $^1A'$ and $^1A''$ PESs, on the other hand, reproduce experimental DCSs, showing that excited electronic states clearly contribute to the dynamics at higher energy.[47,99] Nevertheless, a similar description[26] was not possible for even larger energies, 25.9 kJ mol^{-1} (0.268 eV), with the authors concluding that further theoretical and experimental work was required.

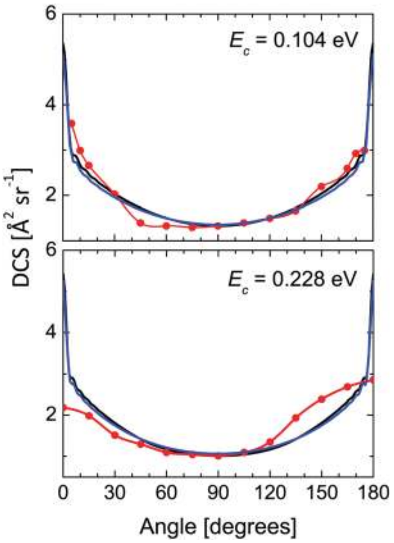

Fig. 3 Differential cross sections for the O(^{1}D) + D$_2$ reaction at 0.104 eV (top) and 0.228 eV (bottom) collision energy. Black lines are present SQM results, blue lines are present MPPST results and red lines are experimental results from Ahmed *et al.*[97] (top) and Alagia *et al.*[18] (bottom), conveniently scaled here to match the theoretical values at the sideways scattering direction, 90 degrees.

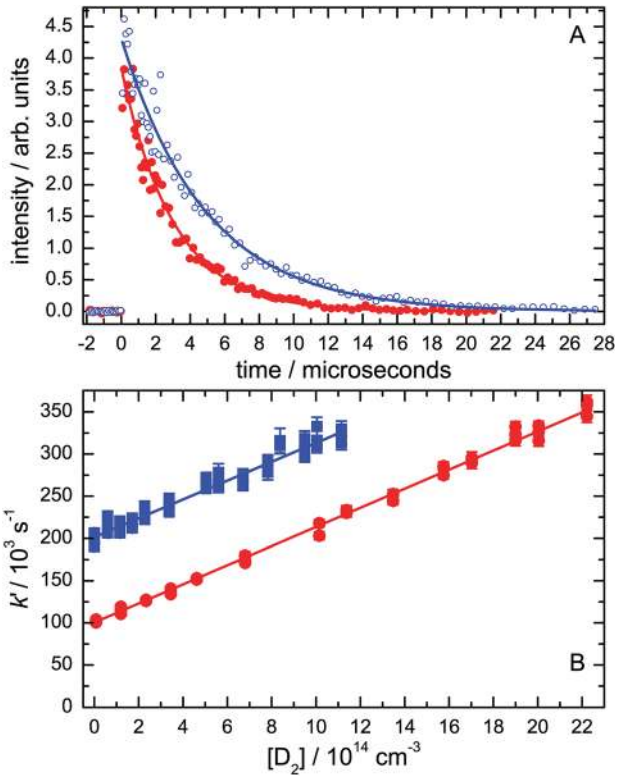

Fig. 4 (A) O(^{1}D) VUV LIF signal as a function of time at 50 K. (red solid circles) [D$_2$] = 1.1 × 10^{15} cm^{-3}; (blue open circles) without D$_2$. The fits are represented by solid blue and red lines using an expression of the form $I_{O(^1D)} = I_{O(^1D)_0}\exp(-k't)$. (B) Measured pseudo-first-order rate constants as a function of [D$_2$]. (red solid circles) 296 K experiments; (blue solid squares) 50 K experiments. Error bars were derived from single-exponential fits to the individual O(^{1}D) decays and are cited at the level of a single standard deviation. Second-order rate constants were derived from weighted fits to the data (solid red and blue lines).

On the experimental side, the O(^{1}D) VUV LIF signal was recorded as a function of time for a range of excess D$_2$ concentrations and in the absence of D$_2$. Two such decay profiles are displayed in Fig. 4A for experiments conducted with [D$_2$] = 1.1 × 10^{15} cm^{-3} and without D$_2$.

In the absence of D$_2$, the O(^{1}D) VUV LIF signal decays exponentially to zero as a function of time through non-reactive quenching collisions with the carrier gas Ar. When D$_2$ is added to the system, O(^{1}D) atoms are removed from the flow by reaction with D$_2$ in addition to quenching by Ar. A function of the type $I_{O(^1D)} = I_{O(^1D)_0}\exp(-k't)$, where t is time and $I_{O(^1D)}$ and $I_{O(^1D)_0}$ are the time dependent and initial O(^{1}D) VUV LIF intensities (which are proportional to the O(^{1}D) concentration) was used to perform a non-linear least-squares fit to the data. This allowed the pseudo-first-order rate constants for

$O(^1D)$ removal, k', to be extracted from the time constants of the decays. In the present experiments, k' is essentially equal to the sum of two contributions (see Grondin *et al.*[75] for a more detailed analysis), $k' = k_{O(^1D)+Ar}[Ar] + k_{O(^1D)+D_2}[D_2]$ where $k_{O(^1D)+Ar}$ and $k_{O(^1D)+D_2}$ are the second-order rate constants for $O(^1D)$ removal by Ar and D_2 respectively. Plotting k' as a function of $[D_2]$ thus allows us to determine $k_{O(^1D)+D_2}$ from a weighted linear least-squares fit to the data. Representative second-order plots obtained at 296 K and at 50 K are shown in Fig. 4B and at 127 K and 75 K in Fig. S3 (ESI†). In these examples, the large y-intercept value represents the quenching contribution of the carrier gas Ar, $k_{O(^1D)+Ar}[Ar]$. The measured second-order rate constants are listed in Table S3 (ESI†) and displayed as a function of temperature in Fig. 5 alongside the present theoretical results and earlier work.

There are several earlier room temperature measurements of the rate constant for the $O(^1D) + D_2$ reaction.[7,12,24,100] The experimental rate constant of $(1.13 \pm 0.11) \times 10^{-10}$ cm^3 s^{-1} determined at 296 K in the present work is in excellent agreement with all but one of these previous investigations.[7] Considering the error bars, the present rate constants are found to be independent of temperature over the 50–296 K range; in good qualitative agreement with our recent investigation of the $O(^1D) + H_2$ reaction over the same range.[16] Fig. 5 also contains the results of previous theoretical investigations of the title reaction.[96,101] Although the results of Pradhan *et al.*[96] were obtained by means of a J-shifting approximation, the good agreement between the present experimental results and both the QM rate constants of Pradhan *et al.*[96] and all the approximate theoretical approaches employed here strongly supports the involvement of a long-lived intermediate complex in the dynamics of the $O(^1D) + D_2$ reaction in this low temperature regime. Interestingly, the rate constants derived by Pradhan *et al.*[96] are approximately 10% lower than the experimental ones, with an identical difference having also been observed in the case of the $O(^1D) + H_2$ reaction.[16,102]

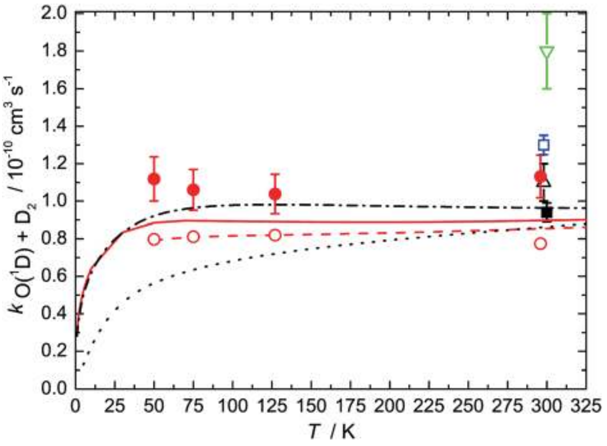

Fig. 5 Rate constants for the $O(^1D) + D_2$ reaction as a function of temperature. Experimental values: (green inverted open triangle) Heidner and Husain;[7] (blue open square) Davidson *et al.*;[100] (black solid square) Matsumi *et al.*;[24] (black open triangle) Talukdar and Ravishankara;[12] (red solid circle) this work. Theoretical values: (dashed dotted black line) QM results of Pradhan *et al.*;[96] (dotted black line) QM results of Sun *et al.*;[101] (solid red line) this work, MPPST method; (dashed red line) this work, SQM method; (red open circles) this work, RPMD method.

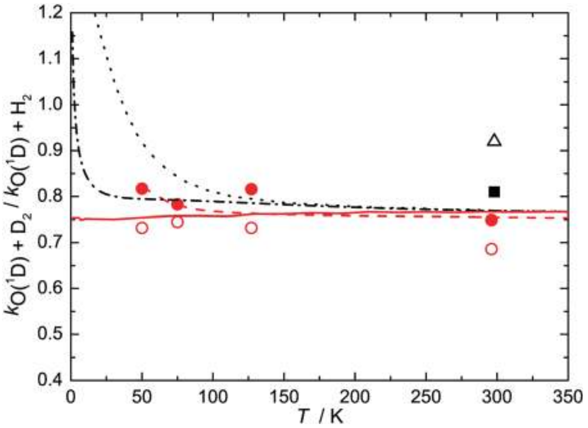

Fig. 6 Kinetic isotope effect (KIE), $k_{O(^1D)+D_2}/k_{O(^1D)+H_2}$, as a function of temperature. Experimental values: (black solid square) Hsu *et al.*;[23] (black open triangle) Talukdar and Ravishankara;[12] (red solid circle) this work. Theoretical values: (dashed dotted black line) QM results of Pradhan *et al.*;[96,102] (dotted black line) QM WP results of Sun *et al.*[101]/QM WP results of Lin and Guo;[44] (solid red line) this work, MPPST method; (dashed red line) this work, SQM method; (red open circles) this work, RPMD method.

As rate constants have already been measured for the $O(^1D) + H_2$ reaction over the same temperature range and calculated using all three theoretical methodologies employed here,[16,45] we can also evaluate the temperature dependent kinetic isotope effect (KIE) (defined as the ratio of the rate constants, $k_{O(^1D)+D_2}/k_{O(^1D)+H_2}$, at a given temperature). The derived KIE values are compared with previous experimental and theoretical work for these systems in Fig. 6.

The present experimental and theoretical KIE values agree very well with the experimental value of 0.81 determined by Hsu *et al.*[23] at higher equivalent temperatures. They are also in excellent agreement above 100 K with the previous theoretical values derived from the ratio of the rate constants obtained by the Sun *et al.*[101] and Lin and Guo[44] QM WP investigations of the $O(^1D) + D_2$ and H_2 reactions respectively over three PESs. While the experimental KIE remains constant down to 50 K, the QM WP KIE increases dramatically below 100 K. This discrepancy could be a sign of convergence issues in either or both QM WP studies at low collision energies. In contrast, the KIE derived by Pradhan *et al.*[96,102] using a time independent QM method and a J-shifting approximation is in excellent agreement with the present experimental and theoretical ones over the entire temperature range.

The comparisons shown in Fig. 5 and 6 between the rate constants (KIE values) derived by exact QM methods and the equivalent values derived by the three theoretical approaches applied here validate the use of these statistical-based and approximate QM methods for an accurate description of the dynamics of complex-forming insertion type reactions in the low temperature regime. The good performance of these classical and statistical approaches suggest that alternative methods such as the statistical QCT method proposed by Aoiz and coworkers[103,104] should also be able to describe the main dynamical features of the title reaction over this temperature range. While such agreement is extremely encouraging, the present and previous calculations all slightly underestimate the measured rate constants for both the $O(^1D) + D_2$ and $O(^1D) + H_2$ reactions at low temperature. These discrepancies could have several possible origins including deficiencies in the PESs used, or they might be due to convergence issues or approximations used during the calculations. Alternatively, such differences could indicate the presence of nonadiabatic couplings in these systems that are not considered by the present calculations. Future work should focus on the inclusion of a correct treatment of nonadiabatic interactions to improve further the agreement between experiment and theory. A possible strategy may comprise calculations including Coriolis coupling between the $1A'$ and $1A''$ PESs, as described by Drukker and Schatz[42] for the case of the $O(^1D) + H_2$ reaction, besides the nonadiabatic contribution coming from the $2A''$ surface.

5 Conclusions

This work presents an experimental and theoretical investigation of the dynamics and kinetics of the gas-phase $O(^1D) + D_2$ reaction. On the experimental side, a supersonic flow reactor was used to attain temperatures as low as 50 K. $O(^1D)$ atoms were produced and detected directly in the cold flow by pulsed laser photolysis and pulsed laser induced fluorescence methods respectively. On the theoretical side, three conceptually different methodologies were used to examine the dynamics of the title reaction – Statistical Quantum Mechanics (SQM), Mean Potential Phase Space Theory (MPPST) and Ring Polymer Molecular Dynamics (RPMD). The results of both the SQM and MPPST calculations confirm that the reaction can be treated statistically and that the dominant mechanism at low temperature involves complex formation through $O(^1D)$ insertion into the D–D bond. Thermal rate constants derived by these two methods are in good agreement with the measured values. Rate constants calculated by RPMD, a more recently proposed method that has no prior assumptions regarding the reaction mechanism, were also in good agreement demonstrating the suitability of this technique for the investigation of insertion reactions down to low temperature. It is argued that the slight discrepancies between theoretical and experimental results could arise either from deficiencies in the present calculations such as approximations or due to inaccuracies in the underlying potential energy surface, or from nonadiabatic effects that are not considered here.

Conflicts of interest

Q5

Acknowledgements

The authors want to thank Prof. Balakrishnan for sharing his QM results. KMH acknowledges support from the French programs ''Physique et Chimie du Milieu Interstellaire'' (PCMI) and ''Programme National de Planétologie'' (PNP) funded by the Centre National de la Recherche Scientifique (CNRS) and Centre National d'Etudes Spatiales (CNES). TGL acknowledges support from MICINN with Grant FIS2014-51993-P and FIS2017-83157-P. Y. V. S. thanks the European Regional Development Fund and the Republic of Cyprus for support through the Research Promotion Foundation (Project Cy-Tera NEA ΥΠΟΔΟΜΗ/ΣΤΡΑΤΗ/0308/31). Y. V. S. also acknowledges the support of the COST CMTS-Action CM1401 (Our Astro-Chemical History).

References

1 M. Agundez and V. Wakelam, Chemistry of Dark Clouds: Databases, Networks, and Models, *Chem. Rev.*, 2013, **113**, 8710–8737.
2 J. W. Stock, C. S. Boxe, R. Lehmann, J. L. Grenfell, A. B. C. Patzer, H. Rauer and Y. L. Yung, Chemical Pathway Analysis of the Martian Atmosphere: CO_2-Formation Pathways, *Icarus*, 2012, **219**, 13–24.
3 D. L. Baulch, Evaluated Kinetic Data for Combustion Modeling: Supplement II, *J. Phys. Chem. Ref. Data*, 2005, **34**, 757–1397.
4 S. P. Sander, J. Abbatt, J. R. Barker, J. B. Burkholder, R. R. Friedl, D. M. Golden, R. E. Huie, C. E. Kolb, M. J. Kurylo, G. K. Moortgat, V. L. Orkin and P. H. Wine, *Chemical Kinetics and Photochemical Data for Use in Atmospheric Studies*, Evaluation No. 17, JPL Publication 10-6, Jet Propulsion Laboratory, Pasadena, 2011, http://jpldataeval.jpl.nasa.gov/.
5 U. Hincelin, V. Wakelam, F. Hersant, S. Guilloteau, J. C. Loison, P. Honvault and J. Troe, Oxygen Depletion in Dense Molecular Clouds: A Clue to a Low O_2 abundance?, *Astron. Astrophys.*, 2011, **530**, A61.
6 J. A. Kernahan and P. H. L. Pang, Experimental Determination of Absolute A Coefficients for 'Forbidden' Atomic Oxygen Lines, *Can. J. Phys.*, 1975, **53**, 455–458.
7 R. F. Heidner and D. Husain, Electronically Excited Oxygen Atoms, $O(2^1D_2)$. A Time-Resolved Study of the Collisional Quenching by the Gases H_2, D_2, CH_4, NO, NO_2, N_2O, and C_3O_2 Using Atomic Absorption Spectroscopy in the Vacuum Ultraviolet, *Int. J. Chem. Kinet.*, 1973, **5**, 819–831.
8 S. T. Amimoto, A. P. Force, R. G. Gulotty and J. R. Wiesenfeld, Collisional Deactivation of $O(2^1D_2)$ by the Atmospheric Gases, *J. Chem. Phys.*, 1979, **71**, 3640–3647.
9 P. H. Wine and A. R. Ravishankara, Kinetics of $O(^1D)$ Interactions with the Atmospheric Gases N_2, N_2O, H_2O, H_2, CO_2, and O_3, *Chem. Phys. Lett.*, 1981, **77**, 103–109.
10 S. Koppe, T. Laurent, P. D. Naik, H. R. Volpp, J. Wolfrum, T. Arusiparpar, I. Bar and S. Rosenwaks, Absolute Rate

Constants and Reactive Cross-Sections for the Reactions of O(^{1}D) with Molecular-Hydrogen and Deuterium, *Chem. Phys. Lett.*, 1993, **214**, 546–552.

11 Y. Matsumi, K. Tonokura, Y. Inagaki and M. Kawasaki, Isotopic Branching Ratios and Translational Energy-Release of H-Atoms and D-Atoms in Reaction of O(^{1}D) Atoms with Alkanes and Alkyl Chlorides, *J. Phys. Chem.*, 1993, **97**, 6816–6821.

12 R. K. Talukdar and A. R. Ravishankara, Rate Coefficients for O(^{1}D) + H_2, D_2, HD Reactions and H Atom Yield in O(^{1}D) + HD Reaction, *Chem. Phys. Lett.*, 1996, **253**, 177–183.

13 J. A. Davidson, H. I. Schiff, G. E. Streit, J. R. McAfee, A. L. Schmeltekopf and C. J. Howard, Temperature Dependence of O(^{1}D) Rate Constants for Reactions with N_2O, H_2, CH_4, HCl, and NH_3, *J. Chem. Phys.*, 1977, **67**, 5021–5025.

14 M. A. Blitz, T. J. Dillon, D. E. Heard, M. J. Pilling and I. D. Trought, Laser Induced Fluorescence Studies of the Reactions of O($^1D_2$) with N_2, O_2, N_2O, CH_4, H_2, CO_2, Ar, Kr and N-C_4H_{10}, *Phys. Chem. Chem. Phys.*, 2004, **6**, 2162–2171.

15 S. Vranckx, J. Peeters and S. Carl, Kinetics of O(^{1}D) + H_2O and O(^{1}D) + H_2: Absolute Rate Coefficients and O(^{3}P) Yields between 227 and 453 K, *Phys. Chem. Chem. Phys.*, 2010, **12**, 9213–9221.

16 K. M. Hickson and Y. V. Suleimanov, Low-Temperature Experimental and Theoretical Rate Constants for the O(^{1}D) + H_2 Reaction, *J. Phys. Chem. A*, 2017, **121**, 1916–1923.

17 R. J. Buss, P. Casavecchia, T. Hirooka, S. J. Sibener and Y. T. Lee, Reactive Scattering of O(^{1}D) + H_2, *Chem. Phys. Lett.*, 1981, **82**, 386–391.

18 M. Alagia, N. Balucani, L. Cartechini, P. Casavecchia, E. H. van Kleef, G. G. Volpi, P. J. Kuntz and J. J. Sloan, Crossed Molecular Beams and Quasiclassical Trajectory Studies of the Reaction O(^{1}D) + H_2(D_2), *J. Chem. Phys.*, 1998, **108**, 6698–6708.

19 X. Liu, C. C. Wang, S. A. Harich and X. Yang, Effect of a Single Quantum Rotational Excitation on State-to-State Dynamics of the O(^{1}D) + H_2 → OH + H Reaction, *Phys. Rev. Lett.*, 2002, **89**, 133201.

20 F. J. Aoiz, L. Bañares, J. F. Castillo, V. J. Herrero, B. Martinez-Haya, P. Honvault, J. M. Launay, X. Liu, J. J. Lin, S. A. Harich, C. C. Wang and X. Yang, The O(^{1}D) + H_2 Reaction at 56 meV Collision Energy: A Comparison between Quantum Mechanical, Quasiclassical Trajectory, and Crossed Beam Results, *J. Chem. Phys.*, 2002, **116**, 10692–10703.

21 S. K. Gray, G. G. Balint-Kurti, G. C. Schatz, J. J. Lin, X. Liu, S. Harich and X. Yang, Probing the Effect of the H_2 Rotational State in O(^{1}D) + H_2 → OH + H: Theoretical Dynamics Including Nonadiabatic Effects and a Crossed Molecular Beam Study, *J. Chem. Phys.*, 2000, **113**, 7330–7344.

22 X. H. Liu, J. J. Lin, S. Harich, G. C. Schatz and X. M. Yang, A Quantum State-Resolved Insertion Reaction: O(^{1}D) + H_2 ($J = 0$) → OH ($^2\Pi$, ν, N) + H(^{2}S), *Science*, 2000, **289**, 1536–1538.

23 Y. T. Hsu, J. H. Wang and K. P. Liu, Reaction Dynamics of O(^{1}D) + H_2, D_2, and HD: Direct Evidence for the Elusive Abstraction Pathway and the Estimation of its Branching, *J. Chem. Phys.*, 1997, **107**, 2351–2356.

24 Y. Matsumi, K. Tonokura, M. Kawasaki and H. L. Kim, Dynamics of the Reaction O(^{1}D) + HD, H_2, and D_2 – Isotopic Branching Ratios and Translational Energy-Release, *J. Phys. Chem.*, 1992, **96**, 10622–10626.

25 P. Hermine, Y. T. Hsu and K. Liu, A Crossed-Beam Study of the Reaction O(^{1}D) + D_2: Collisional Energy Dependence of Differential Cross-Section, *Phys. Chem. Chem. Phys.*, 2000, **2**, 581–587.

26 N. Balucani, P. Casavecchia, F. J. Aoiz, L. Bañares, J. F. Castillo and V. J. Herrero, Dynamics of the O(^{1}D) + D_2 Reaction: A Comparison between Crossed Molecular Beam Experiments and Quasiclassical Trajectory Calculations on the Lowest Three Potential Energy Surfaces, *Mol. Phys.*, 2005, **103**, 1703–1714.

27 S. Kauczok, C. Maul, A. I. Chichinin and K. H. Gericke, Measurement of the Differential Cross Section of the Photoinitiated Reactive Collision of O(^{1}D) + D_2 Using Only One Molecular Beam: A Study by Three Dimensional Velocity Mapping, *J. Chem. Phys.*, 2010, **132**, 244308.

28 X. Liu, J. J. Lin, S. A. Harich and X. Yang, State-to-state Dynamics for O(^{1}D) + D_2 → OD + D: Evidence for a Collinear Abstraction Mechanism, *Phys. Rev. Lett.*, 2001, **86**, 408–411.

29 Y. F. Liu, Y. L. Gao, D. H. Shi and J. F. Sun, Theoretical Study of the Stereodynamics of the Reactions O(^{1}D) + H_2, D_2 and HD, *Chem. Phys.*, 2009, **364**, 46–50.

30 D. Kuang, T. Y. Chen, W. P. Zhang, N. J. Zhao and D. J. Wang, Effects of Reagent Rotation on Stereodynamics Information of the Reaction O(^{1}D) + H_2 ($\nu = 0, j = 0$–5) → OH + H: A Theoretical Study, *Bull. Korean Chem. Soc.*, 2010, **31**, 2841–2848.

31 S. Y. Lin and H. Guo, Energy Dependence of Differential and Integral Cross Sections for O(^{1}D) + H_2 ($\nu = 0, j = 0$) → OH (v',j') + H Reaction, *J. Chem. Phys.*, 2008, **129**, 124311.

32 C. M. A. Rio and J. Brandão, Dynamical Studies and Product Analysis of O(^{1}D) + H_2/D_2 Reactions, *Mol. Phys.*, 2007, **105**, 359–373.

33 M. H. Alexander, E. J. Rackham and D. E. Manolopoulos, Product Multiplet Branching in the O(^{1}D) + H_2 → OH($^2\Pi$) + H Reaction, *J. Chem. Phys.*, 2004, **121**, 5221–5235.

34 J. Hernando, R. Sayos and M. González, A QCT Study of the Microscopic Mechanisms Proceeding via the Ground PES of the O(^{1}D) + H_2 ($X^1\ \Sigma_g^+$) → OH($X^2\ \Pi$) + H(^{2}S) Reaction, *Chem. Phys. Lett.*, 2003, **380**, 123–134.

35 T. Takayanagi, Nonadiabatic Quantum Reactive Scattering Calculations for the O(^{1}D) + H_2, D_2, and HD Reactions on the Lowest Three Potential Energy Surfaces, *J. Chem. Phys.*, 2002, **116**, 2439–2446.

36 T. E. Carroll and E. M. Goldfield, Coriolis-Coupled Quantum Dynamics for O(^{1}D) + H_2 → OH + H, *J. Phys. Chem. A*, 2001, **105**, 2251–2256.

37 P. Honvault and J. M. Launay, A Quantum-Mechanical Study of the Dynamics of the O(^{1}D) + H_2 → OH + H Insertion Reaction, *J. Chem. Phys.*, 2001, **114**, 1057–1059.

38 M. Hankel, G. G. Balint-Kurti and S. K. Gray, Quantum Mechanical Calculation of Product State Distributions for the O(^{1}D) + H_2 → OH + H Reaction on the Ground Electronic State Surface, *J. Chem. Phys.*, 2000, **113**, 9658–9667.

39 A. J. Alexander, F. J. Aoiz, L. Bañares, M. Brouard and J. P. Simons, Product Rotational Angular Momentum Polarization in the Reaction O($^1D_2$) + H_2 → OH + H, *Phys. Chem. Chem. Phys.*, 2000, **2**, 571–580.

40 S. K. Gray, E. M. Goldfield, G. C. Schatz and G. G. Balint-Kurti, Helicity Decoupled Quantum Dynamics and Capture Model Cross Sections and Rate Constants for O(^{1}D) + H_2 → OH + H, *Phys. Chem. Chem. Phys.*, 1999, **1**, 1141–1148.

41 S. K. Gray, C. Petrongolo, K. Drukker and G. C. Schatz, Quantum Wave Packet Study of Nonadiabatic Effects in O(^{1}D) + H_2 → OH + H, *J. Phys. Chem. A*, 1999, **103**, 9448–9459.

42 K. Drukker and G. C. Schatz, Quantum Scattering Study of Electronic Coriolis and Nonadiabatic Coupling Effects in O(^{1}D) + H_2 → OH + H, *J. Chem. Phys.*, 1999, **111**, 2451–2463.

43 Y. Li, Y. V. Suleimanov and H. Guo, Ring-Polymer Molecular Dynamics Rate Coefficient Calculations for Insertion Reactions: X + H_2 → HX + H (X = N, O), *J. Phys. Chem. Lett.*, 2014, **5**, 700–705.

44 S. Y. Lin and H. Guo, Adiabatic and Nonadiabatic State-to-State Quantum Dynamics for O(^{1}D) + H_2(X^1 Σ_g^+, $v_i = j_i = 0$) → OH(X 2Π, v_f, j_f) + H(^{2}S) Reaction, *J. Phys. Chem. A*, 2009, **113**, 4285–4293.

45 A. Rivero-Santamaria, M. L. González-Martínez, T. González-Lezana, J. Rubayo-Soneira, L. Bonnet and P. Larrégaray, The O(^{1}D) + H_2 (X $^1\Sigma^+$, v, j) → OH(X $^2\Pi$, v', j') + H(^{2}S) Reaction at Low Collision Energy: When a Simple Statistical Description of the Dynamics Works, *Phys. Chem. Chem. Phys.*, 2011, **13**, 8136–8139.

46 E. J. Rackham, F. Huarte-Larrañaga and D. E. Manolopoulos, Coupled-Channel Statistical Theory of the N(^{2}D) + H_2 and O(^{1}D) + H_2 Insertion Reactions, *Chem. Phys. Lett.*, 2001, **343**, 356–364.

47 F. J. Aoiz, L. Bañares, J. F. Castillo, M. Brouard, W. Denzer, C. Vallance, P. Honvault, J. M. Launay, A. J. Dobbyn and P. J. Knowles, Insertion and Abstraction Pathways in the Reaction O($^1D_2$) + H_2 → OH + H, *Phys. Rev. Lett.*, 2001, **86**, 1729–1732.

48 P. Larrégaray and L. Bonnet, Rationalizing the S(^{1}D) + H_2 → SH(X $^2\Pi$) + H Reaction Dynamics through a Semi-classical Capture Model, *Comput. Theor. Chem.*, 2012, **990**, 18–22.

49 P. Langevin, Une Formule Fondamentale de Théorie Cinétique, *Ann. Chim. Phys.*, 1905, **5**, 245–288.

50 M. S. Child, *Semiclassical Mechanics with Molecular Applications*, Clarendon Press, Oxford, 1991.

51 R. Meana-Paneda, D. G. Truhlar and A. Fernandez-Ramos, Least-Action Tunneling Transmission Coefficient for Polyatomic Reactions, *J. Chem. Theory Comput.*, 2010, **6**, 6–17.

52 E. J. Rackham, T. González-Lezana and D. E. Manolopoulos, A Rigorous Test of the Statistical Model for Atom-Diatom Insertion Reactions, *J. Chem. Phys.*, 2003, **119**, 12895–12907.

53 T. González-Lezana, Statistical Quantum Studies on Insertion Reactions, *Int. Rev. Phys. Chem.*, 2007, **26**, 29–91.

54 I. R. Craig and D. E. Manolopoulos, Quantum Statistics and Classical Mechanics: Real Time Correlation Functions from Ring Polymer Molecular Dynamics, *J. Chem. Phys.*, 2004, **121**, 3368–3373.

55 S. Habershon, D. E. Manolopoulos, T. E. Markland and T. F. Miller III, Ring-polymer molecular dynamics: Quantum effects in chemical dynamics from classical trajectories in a extended phase space, *Annu. Rev. Phys. Chem.*, 2013, **64**, 387–413.

56 Y. V. Suleimanov, F. J. Aoiz and H. Guo, Chemical Reaction Rate Coefficients from Ring Polymer Molecular Dynamics: Theory and Practical Applications, *J. Phys. Chem. A*, 2016, **120**, 8488–8502.

57 R. Collepardo-Guevara, Y. V. Suleimanov and D. E. Manolopoulos, Bimolecular Reaction Rates from Ring Polymer Molecular Dynamics, *J. Chem. Phys.*, 2009, **130**, 174713.

58 R. Collepardo-Guevara, Y. V. Suleimanov and D. E. Manolopoulos, ''Erratum: Bimolecular Reaction Rates from Ring Polymer Molecular Dynamics'' [*J. Chem. Phys.* 2009, **130**, 174713], *J. Chem. Phys.*, 2010, **133**, 049902.

59 Y. V. Suleimanov, R. Collepardo-Guevara and D. E. Manolopoulos, Bimolecular Reaction Rates from Ring Polymer Molecular Dynamics:Application to H + CH_4 → H_2 + CH_3, *J. Chem. Phys.*, 2011, **134**, 044131.

60 R. Pérez de Tudela, F. J. Aoiz, Y. V. Suleimanov and D. E. Manolopoulos, Chemical Reaction Rates from Ring Polymer Molecular Dynamics: Zero Point Energy Conservation in Mu + H_2 → MuH + H, *J. Phys. Chem. Lett.*, 2012, **3**, 493–497.

61 Y. V. Suleimanov, R. P. de Tudela, P. G. Jambrina, J. F. Castillo, V. Saez-Rabanos, D. E. Manolopoulos and F. J. Aoiz, A Ring Polymer Molecular Dynamics Study of the Isotopologues of the H + H_2 Reaction, *Phys. Chem. Chem. Phys.*, 2013, **15**, 3655–3665.

62 J. W. Allen, W. H. Green, Y. Li, H. Guo and Y. V. Suleimanov, Communication: Full Dimensional Quantum Rate Coefficients and Kinetic Isotope Effects from Ring Polymer Molecular Dynamics for a Seven-Atom Reaction OH + CH_4 → CH_3 + H_2O, *J. Chem. Phys.*, 2013, **138**, 221103.

63 Y. Li, Y. V. Suleimanov, J. Li, W. H. Green and H. Guo, Rate Coefficients and Kinetic Isotope Effects of the X + CH_4 → CH_3 + HX (X = H, D, Mu) Reactions from Ring Polymer Molecular Dynamics, *J. Chem. Phys.*, 2013, **138**, 094307.

64 R. Pérez de Tudela, Y. V. Suleimanov, J. O. Richardson, V. Saéz Rábanos, W. H. Green and F. J. Aoiz, Stress Test for Quantum Dynamics Approximations: Deep Tunneling in the Muonium Exchange Reaction D + HMu → DMu + H, *J. Phys. Chem. Lett.*, 2014, **5**, 4219–4224.

65 E. González-Lavado, J. C. Corchado, Y. V. Suleimanov, W. H. Green and J. Espinosa-Garcia, Theoretical Kinetics Study of the O(^{3}P) + CH_4/CD_4 Hydrogen Abstraction Reaction: The Role of Anharmonicity, Recrossing Effects, and

Quantum Mechanical Tunneling, *J. Phys. Chem. A*, 2014, **118**, 3243–3252.

66 J. Espinosa-García, A. Fernández-Ramos, Y. V. Suleimanov and J. C. Corchado, Theoretical Kinetics Study of the F(^{2}P) + NH_3 Hydrogen Abstraction Reaction, *J. Phys. Chem. A*, 2014, **118**, 554–560.

67 Y. Li, Y. V. Suleimanov, W. H. Green and H. Guo, Quantum Rate Coefficients and Kinetic Isotope Effect for the Reaction $Cl + CH_4 \rightarrow HCl + CH_3$ from Ring Polymer Molecular Dynamics, *J. Phys. Chem. A*, 2014, **118**, 1989–1996.

68 Y. V. Suleimanov and J. Espinosa-García, Recrossing and Tunneling in the Kinetics Study of the $OH + CH_4 \rightarrow H_2O + CH_3$ Reaction, *J. Phys. Chem. B*, 2016, **120**, 1418–1428.

69 Y. V. Suleimanov, W. J. Kong, H. Guo and W. H. Green, Ring-Polymer Molecular Dynamics: Rate Coefficient Calculations for Energetically Symmetric (Near Thermoneutral) Insertion Reactions $(X + H_2) \rightarrow HX + H(X = C(^1D), S(^1D))$, *J. Chem. Phys.*, 2014, **141**, 244103.

70 K. M. Hickson, J.-C. Loison, H. Guo and Y. V. Suleimanov, Ring-Polymer Molecular Dynamics for the Prediction of Low-Temperature Rates: An Investigation of the $C(^1D) + H_2$ Reaction, *J. Phys. Chem. Lett.*, 2015, **6**, 4194–4199.

71 K. M. Hickson and Y. V. Suleimanov, An Experimental and Theoretical Investigation of the $C(^1D) + D_2$ Reaction, *Phys. Chem. Chem. Phys.*, 2017, **19**, 480–486.

72 J. Espinosa-García, C. Rangel and Y. V. Suleimanov, Kinetics Study of the $CN + CH_4$ Hydrogen Abstraction Reaction based on a New Ab Initio Analytical Full-Dimensional Potential Energy Surface, *Phys. Chem. Chem. Phys.*, 2017, **19**, 19341–19351.

73 J. F. Castillo and Y. V. Suleimanov, A ring polymer molecular dynamics study of the $OH + H_2$ (D_2) reaction, *Phys. Chem. Chem. Phys.*, 2017, **19**, 29170–29176.

74 F. J. Aoiz, L. Bañares, J. F. Castillo, V. J. Herrero and B. Martínez-Haya, A Quasiclassical Trajectory and Quantum Mechanical Study of the $O(^1D) + D_2$ Reaction Dynamics. Comparison with High Resolution Molecular Beam Experiments, *Phys. Chem. Chem. Phys.*, 2002, **4**, 4379–4385.

75 R. Grondin, J.-C. Loison and K. M. Hickson, Low Temperature Rate Constants for the Reactions of $O(^1D)$ with N_2, O_2 and Ar, *J. Phys. Chem. A*, 2016, **120**, 4838–4844.

76 N. Daugey, P. Caubet, B. Retail, M. Costes, A. Bergeat and G. Dorthe, Kinetic Measurements on Methylidyne Radical Reactions with Several Hydrocarbons at Low Temperatures, *Phys. Chem. Chem. Phys.*, 2005, **7**, 2921–2927.

77 N. Daugey, P. Caubet, A. Bergeat, M. Costes and K. M. Hickson, Reaction Kinetics to Low Temperatures. Dicarbon + Acetylene, Methylacetylene, Allene and Propene from $77 \leq T \leq 296$ K, *Phys. Chem. Chem. Phys.*, 2008, **10**, 729–737.

78 R. J. Shannon, C. Cossou, J.-C. Loison, P. Caubet, N. Balucani, P. W. Seakins, V. Wakelam and K. M. Hickson, The Fast $C(^3P) + CH_3OH$ Reaction as an Efficient Loss Process for Gas-Phase Interstellar Methanol, *RSC Adv.*, 2014, **4**, 26342–26353.

79 J. Bourgalais, M. Capron, R. K. A. Kailasanathan, D. L. Osborn, K. M. Hickson, J.-C. Loison, V. Wakelam, F. Goulay and S. D. Le Picard, The $C(^3P) + NH_3$ Reaction in Interstellar Chemistry. I. Investigation of the Product Formation Channels, *Astrophys. J.*, 2015, **812**, 106.

80 K. M. Hickson, J.-C. Loison, J. Bourgalais, M. Capron, S. D. Le Picard, F. Goulay and V. Wakelam, The $C(^3P)$ + NH_3 Reaction in Interstellar Chemistry. II. Low Temperature Rate Constants and Modeling of NH, NH_2, and NH_3 Abundances in Dense Interstellar Clouds, *Astrophys. J.*, 2015, **812**, 107.

81 K. M. Hickson, J.-C. Loison, F. Lique and J. Kłos, An Experimental and Theoretical Investigation of the $C(^1D)$ + $N_2 \rightarrow C(^3P) + N_2$ Quenching Reaction at Low Temperature, *J. Phys. Chem. A*, 2016, **120**, 2504–2513.

82 K. M. Hickson, J.-C. Loison, D. Nuñez-Reyes and R. Méreau, Quantum Tunneling Enhancement of the C + H_2O and C + D_2O Reactions at Low Temperature, *J. Phys. Chem. Lett.*, 2016, **7**, 3641–3646.

83 K. M. Hickson, J.-C. Loison and V. Wakelam, Temperature Dependent Product Yields for the Spin Forbidden Singlet Channel of the $C(^3P) + C_2H_2$ Reaction, *Chem. Phys. Lett.*, 2016, **659**, 70–75.

84 D. Nuñez-Reyes and K. M. Hickson, Kinetic and Product Study of the Reactions of $C(^1D)$ with CH_4 and C_2H_6 at Low Temperature, *J. Phys. Chem. A*, 2017, **121**, 3851–3857.

85 Q. Y. Meng, K. M. Hickson, K. J. Shao, J.-C. Loison and D. H. Zhang, Theoretical and Experimental Investigations of Rate Coefficients of $O(^1D) + CH_4$ at Low Temperature, *Phys. Chem. Chem. Phys.*, 2016, **18**, 29286–29292.

86 D. Nuñez-Reyes and K. M. Hickson, The Reactivity of $C(^1D)$ with Oxygen Bearing Molecules NO and O_2 at Low Temperature, *Chem. Phys. Lett.*, 2017, **687**, 330–335.

87 P. Bargueño, T. González-Lezana, P. Larrégaray, L. Bonnet and J.-C. Rayez, Time Dependent Wave Packet and Statistical Calculations on the $H + O_2$ Reaction, *Phys. Chem. Chem. Phys.*, 2007, **9**, 1127–1137.

88 P. Bargueño, T. González-Lezana, P. Larrégaray, L. Bonnet, J.-C. Rayez, M. Hankel, S. C. Smith and A. J. H. M. Meijer, Study of the H + O2 reaction by means of quantum mechanical and statistical approaches: The dynamics on two different potential energy surfaces, *J. Chem. Phys.*, 2008, **128**, 244308.

89 A. J. Dobbyn and P. J. Knowles, A Comparative Study of Methods for Describing Non-adiabatic Coupling: Diabatic Representation of the $^1\Sigma^+/^1\Pi$ HOH and HHO Conical Intersections, *Mol. Phys.*, 1997, **91**, 1107–1124.

90 A. J. Dobbyn and P. J. Knowles, General Discussion, *Faraday Discuss.*, 1998, **110**, 247.

91 P. Larrégaray, L. Bonnet and J.-C. Rayez, Validity of Phase Space Theory for Atom–Diatom Insertion Reactions, *J. Phys. Chem. A*, 2006, **110**, 1552–1560.

92 P. Larrégaray, L. Bonnet and J.-C. Rayez, Mean Potential Phase Space Theory of Chemical Reactions, *J. Chem. Phys.*, 2007, **127**, 084308.

93 Y. V. Suleimanov, J. W. Allen and W. H. Green, RPMD rate: Bimolecular Chemical Reaction Rates from Ring Polymer Molecular Dynamics, *Comput. Phys. Commun.*, 2013, **184**, 833–840.

94 C. H. Bennett, in *Algorithms for Chemical Computations*, ed. R. E. Christofferson, ACS Symposium Series No. 46, American Chemical Society, Washington, DC, 1977, p. 63.

95 D. Chandler, Statistical Mechanics of Isomerization Dynamics in Liquids and the Transition State Approximation, *J. Chem. Phys.*, 1978, **68**, 2959–2970.

96 G. B. Pradhan, N. Balakrishnan and B. K. Kendrick, Quantum Dynamics of $O(^1D) + D_2$ Reaction: Isotope and Vibrational Excitation Effects, *J. Phys. B: At., Mol. Opt. Phys.*, 2014, **47**, 135202.

97 M. Ahmed, D. S. Peterka and A. G. Suits, Crossed-beam Reaction of $O(^1D) + D_2 \rightarrow OD + D$ by Velocity Map Imaging, *Chem. Phys. Lett.*, 1999, **301**, 372–378.

98 J. Brandão and C. M. A. Río, Quasiclassical and Capture Studies on the $O(^1D) + H_2 \rightarrow OH + H$ Reaction using a New Potential Energy Surface for H_2O, *Chem. Phys. Lett.*, 2003, **377**, 523–529.

99 P. Casavecchia, Chemical Reaction Dynamics with Molecular Beams, *Rep. Prog. Phys.*, 2000, **63**, 355–414.

100 J. A. Davidson, C. M. Sadowski, H. I. Schiff, G. E. Streit, C. J. Howard, D. A. Jennings and A. L. Schmeltekopf, Absolute Rate Constant Determinations for the Deactivation of $O(^1D)$ by Time Resolved Decay of $O(^1D) \rightarrow O(^3P)$ Emission, *J. Chem. Phys.*, 1976, **64**, 57–62.

101 Z. P. Sun, S. Y. Lin and Y. J. Zheng, Adiabatic and Non-Adiabatic Quantum Dynamics Calculation of $O(^1D) + D_2 \rightarrow OD + D$ Reaction, *J. Chem. Phys.*, 2011, **135**, 234301.

102 G. B. Pradhan, N. Balakrishnan and B. K. Kendrick, Ultracold Collisions of $O(^1D)$ and H_2: The Effects of H_2 Vibrational Excitation on the Production of Vibrationally and Rotationally Excited OH, *J. Chem. Phys.*, 2013, **138**, 164310.

103 F. J. Aoiz, V. Saéz Rábanos, T. González-Lezana and D. E. Manolopoulos, A Statistical Quasiclassical Trajectory Model for Atom-Diatom Insertion Reactions, *J. Chem. Phys.*, 2007, **126**, 161101.

104 F. J. Aoiz, T. González-Lezana and V. Saéz Rábanos, Stringent Test of the Statistical Quasiclassical Trajectory Model for the H_3^+ Exchange Reaction, *J. Chem. Phys.*, 2007, **127**, 174109.